



HAL
open science

Phase transition in an out-of-equilibrium monolayer of dipolar vibrated grains

Loreto Oyarte, Pablo Gutiérrez, Sébastien Aumaître, Nicolás Mujica

► **To cite this version:**

Loreto Oyarte, Pablo Gutiérrez, Sébastien Aumaître, Nicolás Mujica. Phase transition in an out-of-equilibrium monolayer of dipolar vibrated grains. *Physical Review E: Statistical, Nonlinear, and Soft Matter Physics*, 2013, 87 (2), pp.22204. 10.1103/PhysRevE.87.022204 . cea-01444138

HAL Id: cea-01444138

<https://cea.hal.science/cea-01444138>

Submitted on 23 Jan 2017

HAL is a multi-disciplinary open access archive for the deposit and dissemination of scientific research documents, whether they are published or not. The documents may come from teaching and research institutions in France or abroad, or from public or private research centers.

L'archive ouverte pluridisciplinaire **HAL**, est destinée au dépôt et à la diffusion de documents scientifiques de niveau recherche, publiés ou non, émanant des établissements d'enseignement et de recherche français ou étrangers, des laboratoires publics ou privés.

Phase Transition in a Out-of-equilibrium Monolayer of Dipolar Vibrated Grains

Loreto Oyarte¹, Pablo Gutiérrez², Sébastien Aumaître^{2*} and Nicolás Mujica³

¹*Departamento de Física, Facultad de Ciencias Básicas,
Universidad Metropolitana de Ciencias de la Educación,
Avenida José Pedro Alessandri 774, Ñuñoa, Santiago, Chile*

²*Service de Physique de l'Etat Condensé, DSM, CEA-Saclay, CNRS, 91191 Gif-sur-Yvette, France*

³*Departamento de Física, Facultad de Ciencias Físicas y Matemáticas,
Universidad del Chile, Avenida Blanco Encalada 2008, Santiago, Chile*

(Dated: July 26, 2012)

We report an experimental study on the transition between a disordered liquid-like state and a ordered solid-like one, in a collection of magnetically interacting macroscopic grains. A monolayer of magnetized particles is vibrated vertically at a moderate density. At high excitation a disordered, liquid-like state is observed. When the driving dimensionless acceleration Γ is quasi-statically reduced, clusters of ordered grains grow below a critical value Γ_c . These clusters have a well defined hexagonal and compact structure. If the driving is subsequently increased, these clusters remain stable up to a higher critical value Γ_1 . Thus, the solid-liquid transition exhibits an hysteresis cycle. However, the lower onset Γ_c is not well defined as it depends strongly on the acceleration ramp speed and also on the magnetic interaction strength. Metastability is observed when the driving is rapidly quenched from high acceleration, $\Gamma > \Gamma_1$, to a low final excitation Γ_f . After this quench, solid clusters nucleate after a time lag τ_o , either immediately ($\tau_o = 0$) or after some time lag ($\tau_o > 0$) that can vary from seconds up to several hundreds of seconds. The immediate growth occurs below a particular acceleration value Γ_s ($\lesssim \Gamma_c$). In all cases, for $t \geq \tau_o$ solid cluster's temporal growth can be phenomenologically described by a stretched exponential law. Finally, by taking into account the finite size of our system and by using simple assumptions we propose an alternative tractable theoretical model that reproduces cluster's growth, but which analytical form is not a stretched exponential law.

PACS numbers: 45.70.-n,05.70.Ln,64.70.Dv

I. INTRODUCTION

Granular matter dissipates energy by friction and inelastic collisions, therefore an external driving is necessary to observe dynamical behaviors. Despite their intrinsic macroscopic and non-equilibrium nature, the resulting excited state, from granular gas to an ordered compact set of grains, often shares similarities with the one of thermal systems described by statistical physics at equilibrium. However, important non-equilibrium features emerge, like the absence of a universal effective temperature, deviations from Fourier's conduction law, spatio-temporal instabilities, the absence of scale separation, and so forth. Granular matter is therefore a good candidate to study non-equilibrium phase transitions between these different excited states [1, 2].

The transition of granular media from liquid-like to solid-like states have been already reported. Under shearing or vertical tapping, monodisperse spheres tend to collectively organize themselves in the most dense crystal state [3–6]. When a monolayer of grains that is confined between two horizontal plates is vibrated vertically, unexpected ordered structures nucleate from the liquid state at high excitation [7–9]. This phase separation is driven by the negative compressibility of the effective two di-

mensional fluid, as in the van der Waals model for molecular fluids [9].

In the present experiment, we are concerned by granular systems where another interaction is added to the usual hard sphere collisions. To do so, we use pre-magnetized spheres. Magnetized spheres have been studied under an external applied magnetic field [10, 11]. When a set of these magnetized spheres, compacted by gravity, is submitted to a vertical magnetic field, the surface of the granular packing is destabilized above a given onset and forms peaks [10]. When a granular gas is submitted to an increasing horizontal magnetic field at a given excitation, a transition to a clustered state is observed [11]. A mixture of magnetic and non-magnetic spheres has been also studied in a configuration similar to ours, but at a lower volume fraction of the magnetic particles and in an horizontal plate with no top lid, which limits the energy injection as the system is kept in a quasi-two-dimensional state. In this mixed system, authors focused on the existence and the growth in time of clusters composed of solely magnetic particles, in the bath of non-magnetic ones, as function of control parameters [12, 13].

In our study, no external field is added and the remanent magnetic moment, present in all the particles, generates a dipolar interaction between them. This kind of 2D dipolar liquid (with 3D magnetostatics) has been extensively studied numerically in order to understand the transition from isolated to branched chains [14–16].

*Corresponding author: sebastien.aumaitre@cea.fr

Compared to our experiments, an important difference is that these numerical studies are performed at equilibrium. Also, they use a lower surface density, $\rho = Nd^2/L^2$ up to 0.4 (where d is the particle diameter, N is the number of particles, and L is the system size). Numerical studies also introduce the reduced temperature $T^* = k_B T / (\mu^2/d^3)$, where μ is the magnetic moment of the sphere and d their diameter. Although it is not easy to estimate it in our experiments, we verified at least that the attractive force between particles with aligned moments is weak. Actually, two particles have to be almost in contact to get an attraction that overcomes their own weight, meaning that $\mu^2/d^3 \sim mgd$, with m their mass and g the gravity acceleration. Therefore T^* can be crudely estimated by $T^* \sim m(A\omega)^2 / (\mu^2/d^3)$, using a granular temperature proportional to the energy per grain provided by a vibration of amplitude A and angular frequency ω , and using $\mu^2/d^3 \sim mgd$. One gets $T^* \sim \Gamma A/d \sim 0.2 - 0.6$, which is actually in the range of temperature accessible numerically. A comparison between experiments and numerical studies seems promising.

Here, we present an experimental study of the behavior of a sub-monolayer of pre-magnetized particles that are confined in a shallow geometry, with a height that is small compared to the horizontal dimensions. The system is therefore quasi-two-dimensional with three-dimensional magnetostatics. The experimental cell is submitted to vertical vibration, the control parameter being the dimensionless acceleration $\Gamma = A\omega^2/g$, which is varied keeping constant the driving frequency ω .

This paper is organized in the following way: a description of our experimental device and procedures is presented in section II. Then, we present first, in section III A, the behavior of the system when the control parameter Γ is *quasi-statically* reduced or increased. Below a critical value of Γ , clusters organize in a hexagonal lattice. An hysteretic behavior is observed whether the acceleration of the cell is increased or decreased. In section III B, we present results starting from a liquid-like state, from which we quench the system into the hysteresis region in order to study the dynamical growth of the ordered phase. After presenting our experimental observations on the dynamical evolution of solid clusters, we show that their growth can be fitted by a stretched exponential law. The evolution of the parameters of this law as function of the quenched acceleration is presented and the values of fitted parameters are discussed. In section IV we present a theoretical model for the solid cluster's growth, taking into account the specificity of our experiment, in particular the conserved number of particles and the constant volume. Our model reproduces well the growth but the analytical form is different to the stretched exponential law. In the last section, part V, we present a discussion of our results as well as our conclusions. Some future perspectives are also outlined.

II. EXPERIMENTAL SETUP AND PROCEDURES

The experimental device, illustrated in Fig.1, is similar to the one presented in references [17, 18]. Stainless steel spheres (type 422) of diameter $d = 1$ mm are confined between two horizontal glass plates, which have an indium titanium oxide, ITO, coating layer to prevent static electricity (resistivity $7.5 \times 10^{-6} \Omega\text{m}$, thickness 25 nm). The dimensions of the cell are: the gap between the plates $h = 1.8d$, and lateral dimensions $L_x = L_y = L = 100d$. The cell is submitted to sinusoidal vibration $z(t) = A \sin(\omega t)$, provided by an electromagnetic shaker. We take care to screen its magnetic field. The cell is illuminated from below by an array light emitting diodes. A camera takes pictures from the top. Typical images are shown in Fig. 2. Almost all particles are tracked using an open source Matlab code [19], which works well for the sub-monolayer surface filling fractions that are used. The cell acceleration, $a(t) = \ddot{z}(t)$, is measured with a piezoelectric accelerometer fixed to the base. Our control parameter is the dimensionless acceleration $\Gamma = A\omega^2/g$. Results presented here have been obtained with filling fraction density $\phi = N\pi d^2/4L_x L_y = 0.59$ ($\rho = 0.75$), where $N = 7500$ is the number of spheres, frequency $f = \omega/2\pi = 100$ Hz, period of base oscillation $P = 1/f = 0.01$ s, and $\Gamma = 3 - 5.3$. We have verified that the phenomenology is not qualitatively affected by the number of particles as long as the system is not too dense.

A major experimental challenge is to keep constant the magnetization of the spheres. Indeed, depending on the magnetization procedure, some shifts occur for the acceleration onset values, although the qualitative behavior of

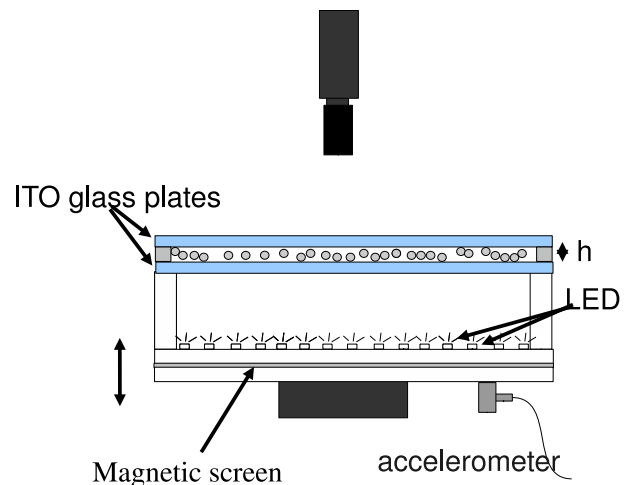


FIG. 1: Sketch of the experimental setup. The cell contains the quasi-two-dimensional box where grains are confined between two ITO coated glass plates. The box is placed above an array of light emitting diodes and a camera pictures the particles from above. An accelerometer measures the applied dimensionless acceleration $\Gamma = A\omega^2/g$.

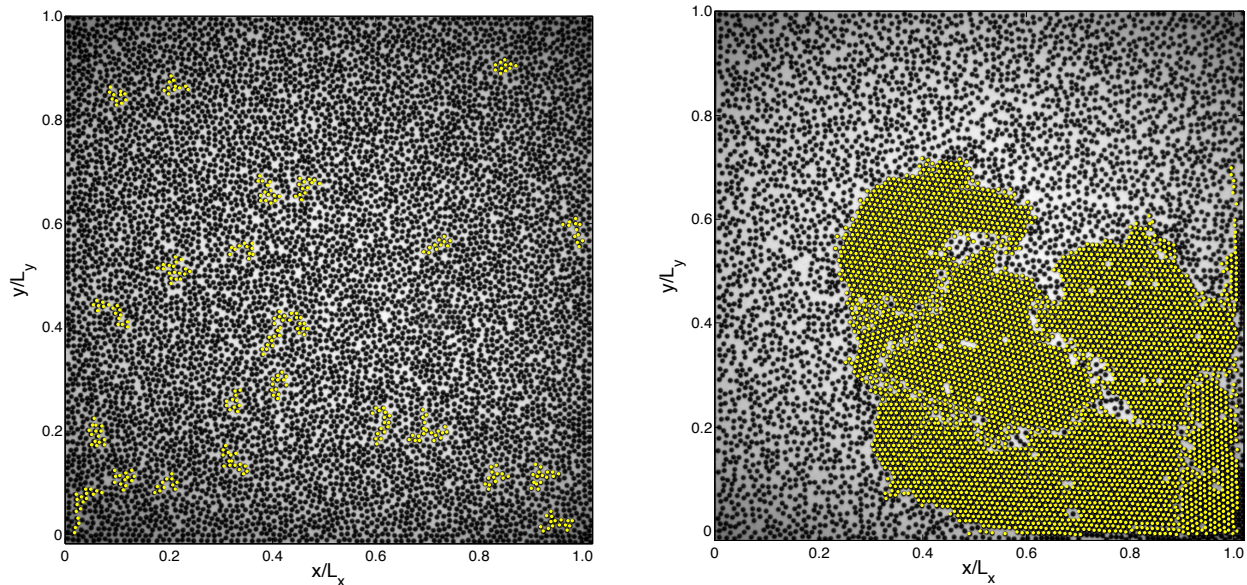


FIG. 2: Left: Disordered liquid state snapshot, $\Gamma = 5$. Yellow dots show groups of more than 10 particles that meet the criterium used for defining particles in a solid cluster. In this liquid state, these clusters are continuously forming and disappearing, tracing density fluctuations. Right: Coexistence of solid and liquid phases, $\Gamma = 3.5$. The solid cluster presents a hexagonal order. It is about two thirds of its final size. Eventually, it will be composed of about 6500 particles, approximately 85% of all particles.

the system remains the same. Grains are magnetized by contact with a strong Neodyme magnet. Some additional thermal treatments have also been probed to maintain the magnetization. The magnetic moment acquired by the spheres is partially lost when the system is vibrated for long times. This loss of interaction strength is produced by collisions and local particle heating. This issue will be discussed in more detail below, in particular when we present experimental results of quasi-static acceleration ramps.

Starting from an homogeneous liquid state at $\Gamma = 5$, and decreasing A for ω fixed, we observe that for $\Gamma \leq 3.5$ clusters of ordered grains grow almost immediately, as shown in Fig. 2-right. In contrast to numerical simulation predictions where all particles form chains [14–16], here clustered particles are well organized in a two dimensional triangular crystal, except at the edge of the cluster where more linear chains coexist with disordered liquid-like particles. In fact, the precise cluster's topology depends on Γ and the speed at which the solid cluster grows. For rapid changes in driving from high acceleration to $\Gamma \sim 1 - 3$, the solid phase will grow quickly and will be first formed by many sub-clusters separated by defects as well as many linear chains. However, if driving is varied slowly from a liquid state, a single cluster will first nucleate and then grow slowly, with a smaller amount of defects, like the one shown in Fig. 2-right.

In order to define the number of particles that are in a solid cluster, N_c , we compute the area of the Delaunay triangle, \mathcal{A} , *i.e.* the area of all the triangles joining the center of each particle with two of this nearest neighbors.

All particles belonging into a Delaunay triangle for which $\mathcal{A} < 0.5d^2$ are defined as belonging to a cluster. The precise value of the onset does not modify qualitatively the results presented here. It has been chosen in order to find all the particles inside a cluster in the cell, as the example shown in Fig. 2-right. Some particles in the liquid phase will inevitably fit this condition as well. This will add a background noise about 1000 particles belonging to small unstable clusters, tracing density fluctuations, like those shown in Fig. 2-left.

III. EXPERIMENTAL RESULTS

A. Quasi-static acceleration ramps

We first present results obtained performing *quasi-static* cooling and heating ramps, by slowly decreasing and increasing the driving acceleration respectively. In Fig. 3, we plot the fraction of particles inside a cluster N_c/N as function of Γ . Blue symbols represent the fraction of crystallized particles when the acceleration is slowly decreased from the liquid state, whereas red ones represent this quantity when the acceleration is slowly increased. Each similar pair of symbols correspond to different experimental realizations. More precisely, the procedure is the following: first the system is set at high acceleration ($\Gamma \approx 5$). The system is left to evolve to a stationary state during a waiting time, t_w . Then, five images are acquired at a rate of 1 fps. Immediately after, Γ is reduced by a small amount and the system is again left

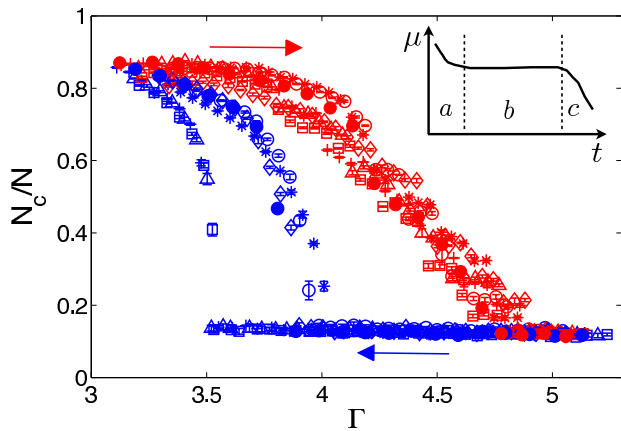


FIG. 3: Total numbers of particles inside a cluster N_c/N as function of Γ . Acceleration is varied *quasi-statically*. Blue (red) symbols indicate the results when Γ is reduced (increased). Several ramps are shown, for different realizations. Each pair of symbols correspond to a closed Γ loop, realized in this order: $\circ, \circ, *, *, \diamond, \diamond, +, +, \triangle, \triangle, \square, \square, \bullet, \bullet$. For each ramp, Γ is varied with a waiting time of 15 s before obtaining images during 5 s at 1 fps. There are two exceptions: ramps for 30 s ($+, +$) and 180 s (\bullet, \bullet) waiting times. Magnetization is reduced after many hours of experiments, evident in some of the the decreasing ramps ($+, \triangle, \square$), were the transition Γ is reduced, although not so in their correspondent increasing ramps ($+, \triangle, \square$). The last two ramps correspond to a longer waiting time (180 s, \bullet, \bullet) for which the transition point again is practically the same as before. Inset: schematic representation of magnetic moment dependence on time.

to evolve during t_w until the next acquisition of images. This procedure is repeated until we reach the lowest acceleration of about $\Gamma = 3.1$. Then, the same procedure is used but increasing Γ until the completely fluidized state is obtained again. For most of the symbols in Fig. 3, $t_w = 15$ s (i.e $t_w = 1500P$). For one case this loop has been realized in the opposite way (symbols \diamond, \diamond in Fig. 3), with no difference in the resulting curves. In two cases, the waiting times are different: ramps with waiting times of 30 s ($t_w = 3000P$: $+, +$) and 180 s ($t_w = 18000P$: \bullet, \bullet). In the caption of Fig. 3, we indicate the order in which these ramps were realized. Particles were not remagnetized during all the experiments presented in this figure.

The inset of Fig. 3 shows an schematic representation of the variation of the average magnetic dipole moment μ with time. Here, “time” means vibration oscillations, *i.e.* time during which the particles are in a fluidized collisional state at a given Γ . Three stages are identified (*a*, *b* and *c*), and the vertical dotted lines indicate the transitions between them. The exact positions of the different transitions depend on Γ and the particular magnetization procedure. Stage *a* is characterized by a fast decrease of μ ; for $\Gamma \sim 5$, this can endure for a few tenths of minutes. Later, stage *b* corresponds to a stable average magnetization, which typically lasts for several hours. And finally,

after many particle collisions, μ continues to decay.

The main result of Fig. 3 is that, for the current cooling and heating rates and procedure, there is a stable loop with two transition points: from an homogeneous liquid to solid-liquid coexistence at $\Gamma_c = 3.9 \pm 0.1$, and from solid-liquid coexistence to the homogeneous liquid state at $\Gamma_l = 4.8 \pm 0.1$. Thus, when the driving is slowly increased, the last cluster disappears always at a critical value which is higher than the value at which the first crystal appears when the driving is decreased: $\Gamma_l > \Gamma_c$. We will refer to this loop as the *quasi-static hysteresis loop* (stage *b*), although it is not reproducible for very long experiments because of a reduction in particle’s magnetization (stage *c*).

Indeed, some curves obtained for decreasing ramps have different Γ_c values as shown by the symbols $+, \triangle$, and \square in Fig. 3. These shifted curves, which result in a lower transition acceleration value ($\Gamma_c \approx 3.5$) from the liquid state to the coexistence of solid and liquid phases, correspond to later runs without remagnetization in between. Therefore, these shifts are mainly due to particle demagnetization. However, for such runs, Γ_l does not change. We remark that when the waiting time t_w is increased to 180 s (18000*P*), symbols \bullet, \bullet in Fig. 3, even with a lower magnetization the previous hysteretic cycle is recovered. It seems that for a lower magnetization and with $t_w = 1500P$ or $t_w = 3000P$, we do not wait enough to obtain the crystal growth. Thus, the loss of magnetization seems to increase the time necessary to get a quasi-stationary state. However, beyond this variability, the main qualitative feature remains: the hysteretic behavior with $\Gamma_c < \Gamma_l$.

Finally, measurements not shown here that are performed just after remagnetization (stage *a*) show that both Γ_c and Γ_l are shifted to higher values, whereas measurements made later, for very long experimental times after magnetization (very late times in stage *c*), present both Γ_c and Γ_l shifted to lower values.

B. Quench experiments

Knowing the onset of crystallization, we now study the dynamics when the homogeneous liquid phase is quenched into a final state near the solid cluster nucleation. Starting from $\Gamma = 5$, we reduce suddenly the driving to a final value Γ_q between 3 and 4.5. We then acquire images at a low frame rate (0.5 fps) for several minutes. The typical measurement time is 10 min ($t_m = 6 \times 10^4P$) in order to keep constant the particle’s magnetic dipole moment during complete run (that is for all the quenches), although some runs with $t_m = 20$ min have also been realized ($t_m = 1.2 \times 10^5P$). For each image, we compute N_c , the total number of particles that belong to a solid cluster.

The temporal evolution of N_c is shown in Fig. 4 for different values of Γ_q . This series of quench experiments was performed in between the quasi-static loops identi-

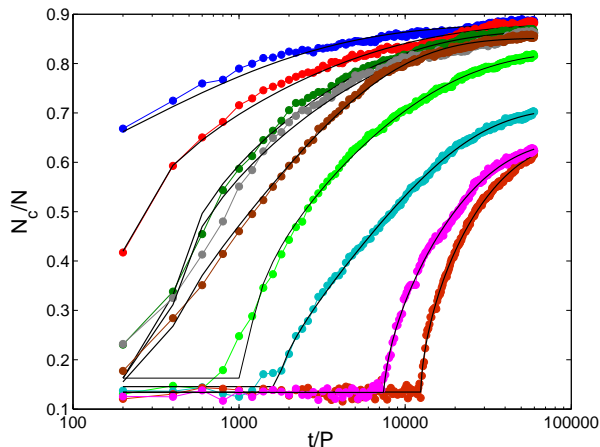


FIG. 4: Number of particles that form part of a solid cluster, N_c/N_o , versus time t/P , for several Γ_q (quenched state). Initial time $t = 0$ corresponds to the moment Γ is abruptly quenched from $\Gamma = 5$ to Γ_q . For each run, images are acquired during 10 min, equivalent to $6 \times 10^4 P$. From left to right $\Gamma_q = 3.15, 3.31, 3.42, 3.53, 3.63, 3.74, 3.94, 4.13$, and 4.02 . For $\Gamma_q = 3.80$ and 4.2 there was no transition within the observation time. Continuous lines show fits for stretched exponential growth law, Eqn. (1). In average, for increasing Γ_q , τ and τ_o increase and N_∞ decreases.

fied by symbols \diamond and $+$ in Fig. 3. Two time scales are clearly present: a growth time τ and a time lag τ_o . Clusters grow slower for higher Γ_q . For $\Gamma_q \lesssim 3.5$, clusters grow immediately ($\tau_o = 0$); for higher Γ_q , cluster's nucleation is delayed ($\tau_o > 0$). This allows us to define for this realization $\Gamma_s \approx 3.5$ as the acceleration below which $\tau_o \approx 0$. In the case $\tau_o > 0$ the system is metastable: it can be either in an homogeneous liquid phase or in a solid-liquid phase separated state. The transition from the former to the latter occurs if there is a density fluctuation strong enough to nucleate crystallization. Additionally, this density fluctuation has to have particles aligned in such a way that they can bound together. As Γ_q approaches Γ_l , this fluctuation has to be stronger (more dense), because the granular temperature is higher. Thus, it becomes less probable too. However, at the same time, its final size is smaller, requesting less bounding energy. The corresponding lag time τ_o becomes usually larger, but its dependence on the appearance of the correct density fluctuation makes it highly variable from one realization to another. The general results is valid for every quench experiment done in the *stable hysteresis loop*: For Γ_q approaching Γ_l , the crystal growth time τ increases, the asymptotic number of particles in the solid phase decreases, and the lag time τ_o seems to increase in average but its variance too (much more independent realizations are needed to study τ_o properly).

In Fig. 4 we also present our data fitted by a stretched exponential growth law

$$N_c(t) = N_\infty + (N_o - N_\infty) \exp[-[(t - \tau_o)/\tau]^\alpha], \quad (1)$$

where N_∞ is the asymptotic number of particles in the solid phase and τ the growth time. N_o is the background “noise” in the measurement of the number of solid particles; in the liquid state, there are many small short-living clusters that are considered as composed by particles in a solid phase, as shown in Fig. 2. Together with the exponent α and time lag τ_o these are used as fit parameters. This stretched exponential law has been used in first order phase transitions to model the growth of the stable phase into the metastable one [20]. It has also been used to describe the compaction of a sand pile under tapping [4]. In our case, the adjustment shown by the continuous lines in Fig. 4 is very good. The exponent α fluctuates around $1/2$ as function of Γ_q , as shown in Fig 5a (data on the x-axis correspond to realizations for which the phase separation was not achieved on the experimental observation time). In fact, the results that are discussed in what follows do not depend strongly on the fact that α can be left as a free parameter or fixed to $\alpha = 0.5$.

The dependence of N_∞ on Γ_q is shown in Fig. 5b. The asymptotic fraction of particles in the solid phase, N_∞/N_c , decreases for high quenching accelerations, from ≈ 0.9 for $\Gamma_q = 3 - 3.4$ to ≈ 0.6 at $\Gamma_q \approx 4$. We notice that except for some experiments where we do not wait enough to overcome the time lag τ_o (data on the x-axis), the value of $N_\infty(\Gamma_q)$ collapses with the one obtained for $N_c(\Gamma)$ by quasi-static heating, showing that we really perform an adiabatic modification of the forcing for the heating case with our quasi-static procedure.

In Figs. 5c and 5d we present τ and τ_o as functions of Γ_q . Our results show that the both times increase strongly in a small range of Γ_q : about two orders of magnitude for Γ_q between 3.1 and 4.1. The longest measured growth and lag times, for $\Gamma_q \approx 4.1$, are $\tau \approx 3.5 \times 10^4 P = 350$ s and $\tau_o \approx 5 \times 10^4 P = 500$ s. If Γ_q is approached to $\Gamma_l = 4.8$, the lag time τ_o becomes larger than the measurement time t_m and no transition from the homogeneous fluid state to the coexistence between solid and fluid phases is observed. In the short parameter range where equation (1) can be verified, we obtain $\tau \sim \exp(a^* \Gamma_q)$, with $a^* = 4.1 \pm 0.5$. Concerning the time lag τ_o , we observe that it is highly variable; much more experiments seem necessary in order to obtain significant statistics. For $\Gamma_q < \Gamma_s = 3.4$, this time lag tends to a constant, $\tau_o \sim 1$ s. As we acquire images at 0.5 fps, this saturation seems artificial. In fact, after doing many realizations we conclude that for $\Gamma_q < \Gamma_s = 3.4$ the solid cluster seems to grow immediately with no delay. Notice that defined this way, Γ_s is different and lower than Γ_c . Thus, our current measurements do not allow us to measure small values of τ_o with enough precision. However, for $\Gamma_q > \Gamma_s = 3.4$, τ_o is a few tenths of seconds, and, despite the poorer statistics, a strong growth is observed. Finally, the strong increases for both τ and τ_o is the reason we can not get closer to Γ_l within the experimental observation times. For example, for $\Gamma_q = 4.5$ and $\Gamma_q = 4.8$, the extrapolation for τ gives $\tau \sim 10^5 P \sim 1000$

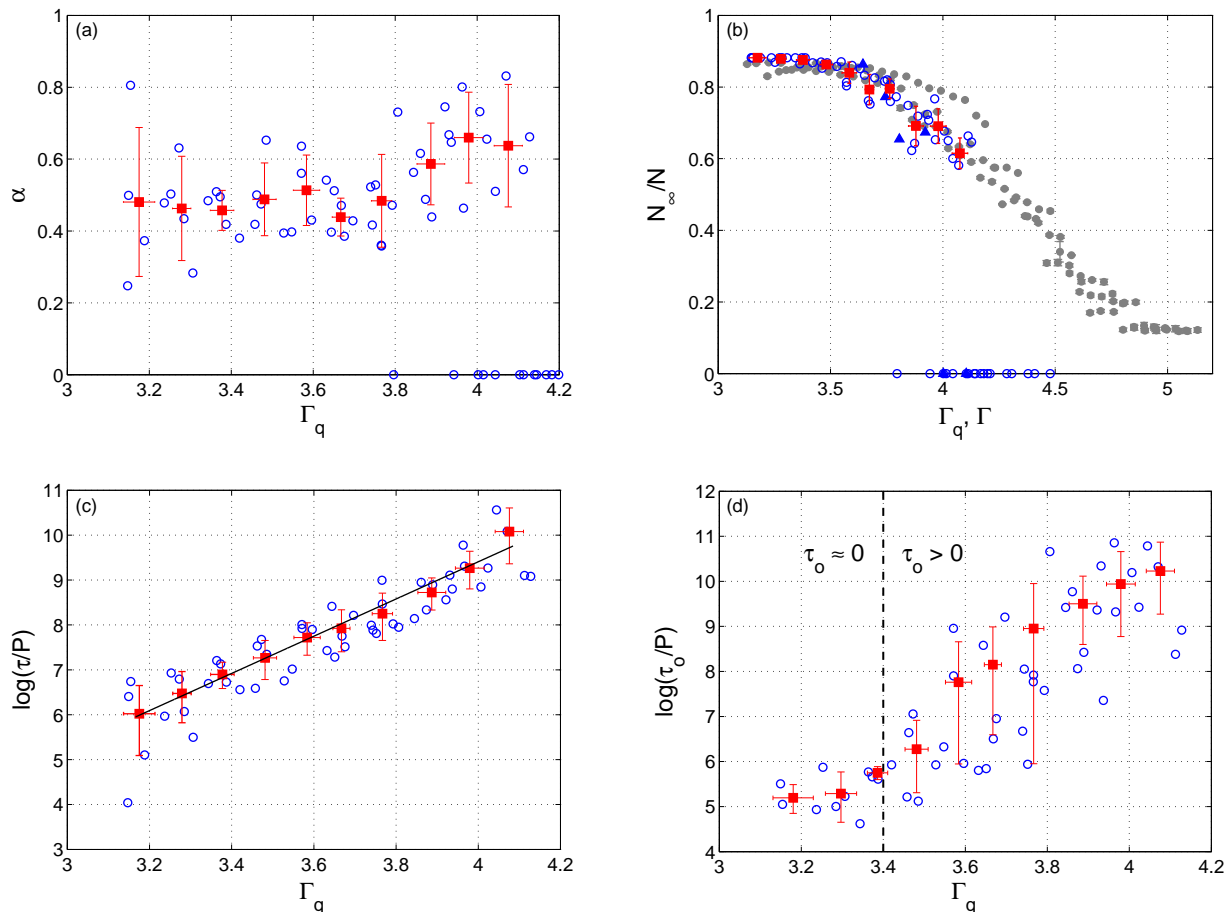


FIG. 5: (Color online) Fitted parameters α (a), N_∞ (b), τ (c) and τ_o (d) as functions of Γ_q . For (a) and (b) symbols on the x-axis correspond to realizations for which the phase separation was not achieved on the experimental observation time. Open circles (\circ) represent raw data obtained from several independent ramps, whereas solid squares (\blacksquare) correspond to averages of data for subsets of Γ_q . Errorbars are computed from standard deviations. In (b), open circles (\circ) have a total measurement time $t_m = 6 \times 10^4 P$, but some data is shown for $t_m = 12 \times 10^4 P$ (\blacktriangle). Solid circles (\bullet) show some of the quasi-static heating curves from Fig. 3. In (c) and (d) the growth time τ and lag time τ_o are plotted in semi-log scale. Both times increase strongly as Γ_l is approached. The continuous line in (c) shows an linear fit $\log(\tau/P) = a^* \Gamma_q + \tilde{a}$, with $a^* = 4.1 \pm 0.5$. The dashed line in (d) indicates the boundary below which clusters grow immediately after a quench.

s and $\tau \sim 4 \times 10^5 P \sim 4000$ s respectively. Because τ_o also would increase significantly, then very long measurement times will be needed and particles would decrease significantly their magnetic interaction strength during these experiments.

IV. DETAILED BALANCE MODEL FOR CRYSTAL GROWTH

In order to model crystal growth in our system, we need to consider a few important considerations: first, the transition occurs at constant volume, which in practice implies a constant surface $L^2 = S_c(t) + S_l(t)$, with $S_c(t)$ the surface occupied by the (2D) solid cluster at time t and $S_l(t)$ the surface available for the disordered liquid phase at that time. Also, the number of parti-

cles is conserved, $N = N_c(t) + N_l(t)$, where $N_l(t)$ is the number particles in the the disordered phase. Secondly, we will consider that clusters grow with a circular shape. Because of the well defined structure of the cluster, once $N_c(t)$ is determined, then $S_c(t)$ is known too. Indeed, they are just related by a geometrical factor: $S_c = \pi R(t)^2$, where $R(t) = b\sqrt{N_c(t)}$ is the mean cluster radius at time t and b a geometrical constant of order of the grains diameter. For instance, for a perfectly ordered crystal in hexagonal close packing one gets

$$\frac{b}{d} = \left(\frac{\sqrt{3}}{2\pi} \right)^{1/2} = 0.53.$$

Next, we can establish a *detailed balance* equation to determine the time evolution of $N_c(t)$. This can be written

$$\frac{dN_c(t)}{dt} = p_{l \rightarrow c} N_l(t) - p_{c \rightarrow l} N_c(t), \quad (2)$$

where $p_{l \rightarrow c}$ is the probability by unit time that a particle of the disordered phase is captured by the solid cluster and $p_{c \rightarrow l}$ is the probability by unit time that a particle escapes from the cluster to the liquid phase. The first can be estimated crudely as the collision frequency between a cluster and the liquid particles which have a velocity small enough to be caught by the former. If we characterize these particles by their mean velocity v_o , we assume

$$p_{l \rightarrow c} \sim \frac{N_l(t)}{S_l(t)} v_o 2R(t)$$

since $2R(t)$ is almost the cross-section of the cluster (for $R(t) \gg d$). Now, particles leaving a cluster have to be at its perimeter. We can assume that they have a constant probability by unit time p to leave this perimeter. Therefore, because for simplicity we consider an almost circular cluster we obtain

$$p_{c \rightarrow l} \sim \frac{2\pi R(t)b}{\pi R(t)^2} p.$$

Both v_o and p would depend on quench acceleration Γ_q , on the distance to Γ_l , that is $\Delta\Gamma = \Gamma_l - \Gamma_q$, on the particle density N/L^2 and on dipole magnetization μ . Knowing the relation between L^2 , $S_l(t)$, $R(t)$, N , $N_l(t)$ and $N_c(t)$ imposed by the constant surface, number of particles and the crystal structure of the clusters, we can rewrite (2) as

$$\frac{dn(\theta)}{d\theta} = \left(\frac{(1-n(\theta))^2}{1-\beta n(\theta)} - \gamma \right) \sqrt{n(\theta)}, \quad (3)$$

where we had introduced the normalized number of particles in the solid cluster, $n(\theta) = N_c(t)/N$, the rescaled time, $\theta = (2\rho v_o b \sqrt{N_o})t$, with $\rho = N/L^2$, the geometrical factor $\beta = \pi b^2 \rho$ and the parameter $\gamma = p/(b\rho v_o N)$. Notice that these parameters are not free fitting parameters. Indeed, the geometric parameter should be $\beta \approx \rho d^2 \sqrt{3}/2 \approx 0.65$. It will be fixed to this value hereafter. Moreover, in the time-asymptotic regime or along the quasi-static heating ramp we can impose $dn(\theta)/d\theta = 0$. Then, the parameter γ is obtained through the the well defined stationary values $n_\infty = N_\infty/N$ shown Fig. 5b. Therefore, for a given value of the quenched acceleration Γ_q , the value of γ is obtained by

$$\gamma = \frac{(1-n_\infty)^2}{1-\beta n_\infty}. \quad (4)$$

The only undetermined parameter is the characteristic velocity v_o , thus the time scale $t^* = (2\rho v_o b \sqrt{N})^{-1}$.

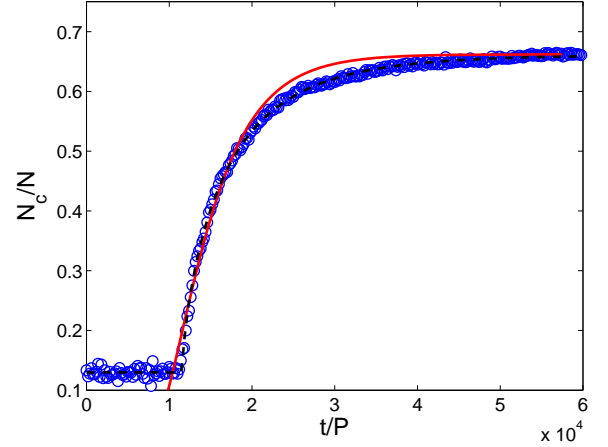


FIG. 6: (color online) The adjustment of experimental results with equation (6) is shown with a continuous curve (red) for $\Gamma_q = 3.92$ for which $N_\infty/N = 0.662$ and $\beta = 0.65$. Fit parameters are the time scale $t^*/P = 4000$ and growth starting time $t_o/P = 6500$. For comparison the dashed line (black) shows the stretched exponential fit given by Eqn. (1), with parameters $N_o/N = 0.130 \pm 0.001$, $N_\infty/N = 0.661 \pm 0.001$, $\alpha = 0.77 \pm 0.02$, $\tau/P = 5350 \pm 80$, and $\tau_o/P = 11520 \pm 50$.

Equation (3) can be solved to obtain the following expression for θ as a function of n :

$$\frac{\theta}{\theta_o} = C_1 \cdot \tanh^{-1} \left(\sqrt{\frac{n}{n_\infty}} \right) - C_2 \cdot \tanh^{-1} \left(\sqrt{\frac{n}{n^*}} \right) \quad (5)$$

$$= \ln \left[\left(\frac{1+\sqrt{n/n_\infty}}{1-\sqrt{n/n_\infty}} \right)^{C_1/2} \cdot \left(\frac{1-\sqrt{n/n^*}}{1+\sqrt{n/n^*}} \right)^{C_2/2} \right] \quad (6)$$

where

$$n^* = \frac{(2-n_\infty-\beta)}{(1-\beta n_\infty)}$$

is the second root (larger than 1) of the polynomial relation issued of (4),

$$C_1 = \frac{(1-\beta n_\infty)}{\sqrt{n_\infty}},$$

$$C_2 = \frac{(1-\beta)^2}{\sqrt{(2-n_\infty-\beta)(1-n_\infty\beta)}},$$

and

$$\theta_o = \frac{2(1-\beta n_\infty)}{(2-n_\infty-\beta)(1-n_\infty\beta)}.$$

Fig. 6 shows that a numerically inverted relation (6) with t^* as a fit parameter reproduces also quite satisfactorily the experimental results. We stress that this fit has only two adjustable parameters, t^* and t_o (the starting growth time), whereas the stretched exponential form has five, N_o , N_∞ , τ , τ_o and α (when α is left as a free parameter).

V. DISCUSSION AND CONCLUSIONS

In summary, quasi-static cooling and heating of a layer of dipolar interacting spheres is performed by slow changes of the driving acceleration. The system exhibits an hysteretic phase transition between a disordered liquid-like phase and an ordered phase. The ordered phase is formed by dense clusters, structured in an hexagonal lattice, coexisting with disordered grains in a liquid-like phase. By quenching the system in the vicinity of the transition, we study the dynamical growth of the ordered clusters, which can arise after a time delay. The time evolution of the number of particles in the solid-crystal phase is well fitted by a stretched exponential law, but also by relation (6) that we have obtained analytically.

The first point to discuss is why we do not observe particles in a state of branched chain, as reported in numerical simulations [14–16]. Indeed our filling fraction, $\phi = 0.59$ as well as the reduced temperature $T^* \sim 0.4$, are not so far from the values used in [14–16]. However, we do not observe the branched state reported in these studies, at least not as a stable, stationary configuration. For our experiment, as mentioned in section II, if a quench is done deeply into the solid phase, $\Gamma_q \sim 1 - 3$, then many small solid clusters are formed quickly and many linear chains are present. However, this state eventually evolves to a more densely packed state, with almost no linear chains, in coexistence with the liquid phase. More systematic experiments should be performed to study properly this aging process.

Compared to numerical simulations, one of the major differences is in the vertical vibration imposed in our experiment to sustain particle motion. Indeed, instead of the 2D thermal motion used in numerical studies, a particle in the solid phase collides the bottom and top plates during an excitation period. The vertical motion might disadvantage the formation of long chains, and compact clusters might be more stable under such driving. Moreover, in contrast to numerical simulations, the magnetic dipole moments are probably not uniformly distributed in all the particles. Although it is really difficult to estimate the width of dipole moments distribution in our experiment, a fraction of them could be small enough to prevent bounding.

The second point deserving discussion is the existence of the quasi-static hysteresis loop when the driving amplitude is slowly modified. A crucial point is that during a cooling ramp there is a specific driving, Γ_c , which depending on the particular magnetization history is between 3.5 and 3.9, below which solid clusters grow. Due to magnetization reduction and because τ and τ_o vary with driving amplitude, this specific boundary is very difficult to determine more precisely. How slow one should vary the driving depends on the time scales that are present in the system, that is on τ and τ_o . The quench experiments show that, within the hysteresis loop, both times grow strongly with driving amplitude. These same

quench experiments show the existence of another particular acceleration Γ_s ($\lesssim \Gamma_c$), below which $\tau_o \approx 0$. This onset value seems to be better defined than Γ_c .

Our quasi-static increasing acceleration ramps show that the heating branch of the loop seems to be a stable, adiabatic branch. In particular, all quasi-static heating ramps follow the same curve and the critical driving above which solid clusters disappear, $\Gamma_l = 4.8 \pm 0.1$, is very reproducible. The fact that we are able to follow adiabatically this stable branch can be understood with the following reasoning:

- A ramp starts at low Γ with a well formed solid cluster (or clusters) in coexistence with the liquid phase;
- The driving amplitude is increased in a small amount, which increases the system’s kinetic energy (granular “temperature”);
- Particles in the solid phase but at the cluster’s boundary will receive stronger collisions from those in the liquid phase, so the probability of getting ripped off increases;
- This results in a cluster size reduction, more or less continuously as the driving is increased further;
- As the change from the one state to another occurs smoothly, the time it takes can be short.

The fact that $\Gamma_l > \Gamma_s$ demonstrates that there is a metastable region for which the system might stay in a completely fluidized state, but from which eventually a solid cluster will nucleate and grow until a stationary size is reached. Also, quench experiments done for $\Gamma_q = 3.4 - 3.9$ show that the final cluster size is the same as the obtained for the heating ramp (N_∞/N collapses with N_c/N of the heating quasi-static loop). This shows that the cooling ramp branch of the quasi-static loop is not stable, implying that the cooling ramp was probably not done slowly enough. This is consistent with the fact that for a given magnetic interaction strength, the value of Γ_c depends on the decreasing ramp rate. As the number of solid particles has to grow from the background noise level to the final asymptotic one, then waiting times much longer than τ_o are necessary. Another possible route for the metastable state characterization would be to study precursors through density and velocity correlations.

We now turn to the values of α used to fit experimental data with a stretched exponential law. At equilibrium, we would expect an exponent $\alpha = D + 1 = 3$ [20], where $D = 2$ is the spatial dimension, but instead we obtain $\alpha \approx 0.5$. Due to the anisotropy of the attractive force, of the special shape of the interface and of the fact that most of the clusters start to grow from boundaries, one could assume that our experiment behaves more like 1D system, but even in this extreme case, we should have get $D \geq 1$ and $\alpha \geq 2$. Moreover, one has to underline that

we are in a out-of-equilibrium dissipative system. Others aspects can therefore play a role, like dissipation, which is probably different in the cluster and liquid phase, or the very particular thermalization imposed by vertical vibration. This effect could be especially important near the transition where a critical behavior can be expected. Actually, an exponent $\alpha < 1$ is measured in another out-of-equilibrium system: the slow compaction of granular packing by tapping [4], but the meaning of such law is still under debate in this case. This issue deserves further studies by changing the boundary shape (from square to circular) or by doing the experiment in a viscous fluid to modify the dissipation or by exciting the grains by vibration using colored noise with a broad frequency range.

It is clear that the present system is strongly out of equilibrium. Despite it can reach stationary states, at coexistence the effective in plane “granular” kinetic temperatures can be very different between the liquid and solid phases. In the metastable region, the transition from the liquid state to the coexisting one can be achieved with the experimental time scales that are available. This transition occurs because the appropriate fluctuation occurs in the liquid state. But, once a particle is trapped in the solid state, specially those deep inside the boundary layer, it is very difficult for them to escape. Indeed, from our model we can estimate in a stationary regime that the ratio between the probability rates $p_{l \rightarrow c}$ and $p_{c \rightarrow l}$ is given by

$$\frac{p_{l \rightarrow c}}{p_{c \rightarrow l}} = \frac{n_\infty}{1 - n_\infty}. \quad (7)$$

For $\Gamma < \Gamma_s$, $p_{l \rightarrow c}/p_{c \rightarrow l} \gtrsim 7$. This allows us to propose that the transition in our system is a good candidate to be considered as quasi-absorbing hysteretic phase transition. However, the relative small size of the system and our imperfect control on the spheres magnetization and therefore on the transition onsets, makes very difficult any quantitative benchmark between our system with other systems exhibiting out-of-equilibrium quasi-absorbing phase transitions. Nonetheless, some promising qualitative similarities can be underlined between our experiment and the out-of-equilibrium transition observed between two turbulent phases of a liquid crystals, transition that belongs to the direct percolation universality class [2]. In this system an hysteresis loop is observed between a turbulent phase stable at high excitation (called DSM2) and a quasi-absorbing state (called DSM1) [21, 22]. Also, an exponential decay of DSM2 phase is observed when it is quenched in the DSM1 stable region [2]. Computations of the critical exponents is beyond the experimental accuracy accessible with our system and procedures and will need a larger device and also a better control of the magnetic interaction strength.

Acknowledgments

We thank Cecile Gasquet, Vincent Padilla and Correntin Coulais for valuable technical help and discussions. This research was supported by grants ECOS-CONICYT C07E07, Fondecyt No. 1120211, Anillo ACT 127, and RTRA-CoMiGs2D.

-
- [1] S. Lübeck, Universal scaling behavior of non-equilibrium phase transition, *Int. J. Mod. Phys. B* **18**–31 & 32, 3977–4118 (2004).
 - [2] K.A. Takeuchi, M. Kuroda, H. Chaté, and M. Sano, Directed Percolation Criticality in Turbulent Liquid Crystals, *Phys. Rev. Lett.* **99**, 234503 (2007).
 - [3] O. Pouliquen, M. Nicolas and P.D. Weidman, Crystallization of non-Brownian Spheres under Horizontal Shaking, *Phys. Rev. Lett.* **79**–19, 3640–3643 (1997).
 - [4] G. Lumay and N. Vandewalle, Experimental Study of Granular Compaction Dynamics at Different Scales: Grain Mobility, Hexagonal Domains, and Packing Fraction, *Phys. Rev. Lett.* **95**, 028002 (2005).
 - [5] S. Živković Z. M. Jakšić, D. Arsenović, Lj. Budinski-Petković, and S. B. Vrhovac, Structural characterization of two-dimensional granular systems during the compaction, *Granular Matter* **13**, 493502 (2011).
 - [6] S. Aumaitre, T. Schnautz, C.A. Kruelle, and I. Rehberg, Granular Phase Transition as a Precondition for Segregation, *Phys. Rev. Lett.* **90**, 114302 (2003).
 - [7] A. Prevost, P. Melby, D. A. Egolf, and J. S. Urbach, Non-equilibrium two-phase coexistence in a confined granular layer, *Phys. Rev. E* **70**, 050301(R) (2004).
 - [8] P. Melby *et al.*, The dynamics of thin vibrated granular layers, *J. Phys. Cond. Mat.* **17**, S2689 (2005).
 - [9] M.G. Clerc, P. Cordero, J. Dunstan, K. Huff, N. Mujica, D. Risso, and G. Varas, Liquid-solid-like transition in quasi-one-dimensional driven granular media, *Nature Physics* **4**, 249 (2008).
 - [10] D. Lopez and F. Pétrelis, Surface Instability Driven by Dipole-Dipole Interactions in a Granular Layer, *Phys. Rev. Lett.* **104**, 158001 (2010).
 - [11] C. Laroche and F. Pétrelis, Observation of the condensation of a gas of interacting grains, *Eur. Phys. J. B* **77**, 489492 (2010).
 - [12] A. Kudrolli and D.L. Blair, Clustering transitions in vibrofluidized magnetized granular materials, *Phys. Rev. E* **67**, 021302 (2003).
 - [13] A. Kudrolli and D.L. Blair, Magnetized Granular Materials, in *The Physics of Granular Media*, edited by H. Hinrichsen and D.E. Wolf (Wiley-VCH, 1st Ed., 2005)
 - [14] T. Tlusty and S. A. Safran, Defect-Induced phase separation in dipolar fluids, *Science* **290**, 1328 (2000).
 - [15] P.D. Duncan and P.J. Camp, Aggregation Kinetics and the Nature of Phase Separation in Two-Dimensional Dipolar Fluids, *Phys. Rev. Lett.* **97**, 107202 (2006).
 - [16] J. M. Tavares J. J. Weis and M. M. Telo da Gama, Phase transition in two-dimensional dipolar fluids at low densities, *Phys. Rev. E* **73**, 041507 (2006).
 - [17] N. Rivas, S. Ponce, B. Gallet, D. Risso, R. Soto, P. Cordero and N. Mujica, Sudden chain energy transfer events in vibrated granular media, *Phys. Rev. Lett.* **106**,

- 088001 (2011).
- [18] G. Castillo, N. Mujica and R. Soto, arXiv:1204.0059v1 (2012).
- [19] D. Blair and E. Dufresne,
<http://physics.georgetown.edu/matlab/>
- [20] M. Avrami, Kinetics of phase change. I General theory, *J. Chem. Phys.* **7**, 1103 (1939). Kinetics of phase change. II Transformation-Time Relations for Random Distribution of Nuclei, *J. Chem. Phys.* **9**, 212 (1940).
- [21] S. Kai, W. Zimmermann, M. Andoh, and N. Chizumi, Local transition to turbulence in electrohydrodynamic convection, *Phys. Rev. Lett.* **64**-10, 1111 (2011)
- [22] K.A. Takeuchi, Scaling of hysteresis loops at phase transitions into a quasiabsorbing state, *Phys. Rev. E* **77**, 030103(R) (2008).